Multi-omic analysis of a microalga after 13 years of acclimation under high-CO_2 for flue gas mitigation and high-value byproduct generation

Shirley Mora-Godínez[1], Carolina Senés-Guerrero[2], Adriana Pacheco[1]
[1]Tecnologico de Monterrey, Escuela de Ingenieria y Ciencias, Monterrey, N.L., Mexico, 64849
[2]Tecnologico de Monterrey, Escuela de Ingenieria y Ciencias, Zapopan, Jalisco, Mexico, 45138
shirleymora@tec.mx, adrianap@tec.mx

Abstract*– Microalgae present high potential for greenhouse gas mitigation and value-added biomass production. In this project, the main objective was to characterize genetic and biochemical changes of high CO_2 (HCA) and low CO_2 (LCA) acclimated strains of Desmodesmus abundans RSM under a model cement flue gas by using genomic, transcriptomic, and lipidomic pipelines. Strain growth under the flue gas was characterized in a N and S-depleted culture medium to evaluate gas components (NO_x and SO_x) as nutrient sources. Draft genomes of D. abundans strains were generated and resulted in an estimated size of 81.20 and 83.61 Mb for HCA and LCA, respectively; and 10 535 and 14 251 predicted genes. Evolution of the strain HCA was characterized by some differentially annotated GO (Gene Ontology) terms compared to LCA. When D. abundans strains were grown under the flue gas condition, HCA strain showed higher initial growth rates and N consumption during the exponential phase than LCA; but similar biomass productivities were reached at the end of the experiment. Also, differences in biomass composition were observed among strains. HCA strain possessed a higher content of pigments (32-44% more chlorophyll a and b, and carotenoids), but lower content of starch and lipids compared to LCA. Differential transcriptome analysis resulted in 16,435 up-regulated and 4,219 down-regulated contigs in HCA compared to the LCA strain. These contigs corresponded mainly to genes involved in nucleotide and amino acid synthesis, carbon fixation, C3 and C4 cycle, glycolysis and gluconeogenesis, and TCA cycle. Lipidome analysis showed higher intensities of putative glycerophospholipids in the HCA strain, while glycerolipids were higher in LCA. Results suggest that D. abundans strains exhibit different levels of adaptability and response to flue gas because of acclimation to different CO_2 concentrations. Understanding the adaptative mechanisms to high CO_2 and response to flue gas could contribute to developing cultivation strategies for microalgae CO_2 mitigation and biotechnology applications.

Keywords*-- Microalgae, Desmodesmus, flue gas, genomic, transcriptomic, lipidomic, byproducts

I. Introduction

Global warming is one of the main environmental global concerns, which has worsened as consequence of greenhouse gas (GHG) emissions [1]. CO_2 is the major GHG since it contributes to 66% of the earth´s radiative forcing, where primary emissions are from fossil fuel combustion and the cement industry [2]. Therefore, there is an urgency in the establishment of biomitigation systems with high CO_2 capture efficiencies. Among photosynthetic organisms, microalgae possess CO_2 fixation rates twelve or more times higher than plants due to their rapid growth [3], [4]. Also, microalgal biomass represents a neutral carbon renewable source for human nutrition and energy production [5], [6], which together with climate action represent important sustainable development goals worldwide [7].

Microalgae are a promising alternative for biological mitigation of CO_2 and carbon revalorization through biomass conversion into added-value byproducts [3], [8], [9], [10]. Microalgae biomass is characterized by a high content of lipids (2-80 %), carbohydrates (11-75 %), protein (10-70 %), and pigments (3-5%) [11], [12], [13], [14]. Some applications of microalgae are biofuel generation, human and animal feed, cosmetic, pharmaceutic, and biofertilizer production, among others [10], [15]. Additionally, these microorganisms possess promising characteristics for industrial applications such as high biomass and metabolite productivities, and no arable land nor freshwater is required for cultivation [4], [16], [17].

Despite microalgae production advantages and efforts in optimizing cultivation and harvesting, production cost is still high (US$3-50 /Kg) [18], [19], [20]. Cost optimization is dependent on biomass productivity [20], which is affected by culture conditions, bioreactor configuration (i.e., raceway, tubular photobioreactor, flat panel, among others), and operation mode such as batch, fed-batch, continuous or semi-continuous cultures [17]. On the other hand, adaptative laboratory evolution protocols have been proposed as a strategy to improve the tolerance and performance of microalgae under certain growth conditions [24]. These adaptations have been related to the accumulation of beneficial mutations/genetic variants [24], [25]. Moreover, only a few microalgae strains have been well characterized in this sense.

In addition, the number of microalgae species worldwide is estimated to be one million, which are present in different habitats and might possess a rich repertoire of metabolic pathways [26]. Of these, only 222 de novo genomes of 149 microalgae species from 97 genera had been reported by January 2020 [27]. Genome sequencing is a promising tool for exploring microalgae metabolism and generating in-depth information about adaptation mechanisms [5]. With the

generated information, microalgae strains could be manipulated by genetic engineering to give rise to highly productive strains with improved contaminant removal rates [28], [29].

Among Chlorophyta microalgae, species from the Scenedesmaceae family have shown to tolerate high CO_2 concentrations with high biomass and metabolite productivities [9], [30], [31], [32]. Genomic analyses have been performed in some of these species [5], [26], [33], [34], [35], [36]. Also, transcriptomic studies have been conducted in *Desmodesmus* species to elucidate pathways of lutein biosynthesis [37] and bisphenol biodegradation [38]; and in *Scenedesmus* species related to lipid metabolism under N depletion [39]. However, genomic studies focused on carbon fixation in these species are limited.

The microalgae in this study, *Desmodesmus abundans* (strain RSM, UTEX 2976), is an environmental microalga isolated in 2008 by our group from a river in Monterrey, Nuevo Leon, Mexico [40]. The strain has been acclimated to high CO_2 (strain HCA, 50% v/v CO_2/air) and low CO_2 (strain LCA, atmospheric, 0.04% v/v CO_2/air) for thirteen years. In previous studies, strain HCA showed higher growth and utilization of cement flue gas components. In the present study, the main objective was to characterize genetic (genome and transcriptome) and biochemical changes of low and high CO_2 adapted microalgae strains (LCA and HCA) to elucidate adaptation mechanisms; as well as to optimize growth under a model cement flue gas mitigation scenario in a 1 L column photobioreactor to improve CO_2 capture and propose high-value byproducts of the system.

II. Materials and Methods

A. Microalgae strains and CO_2 acclimation strategies

The microalgae, *Desmodesmus abundans* strain RSM (UTEX 2976) was isolated from a freshwater river (pH 7.4) in the city of Monterrey, Nuevo Leon, Mexico, in 2008 by our research group. The strain was obtained after sample enrichment under air for one month and, then acclimated to 25 % v/v CO_2/air (Fig 1). After six months, the culture was exposed to an atmosphere of 50 % v/v CO_2/air. Cultures have been maintained under air (low CO_2 acclimated, LCA strain) and 50% v/v CO_2/air (high CO_2 acclimated, HCA strain) for 13 years. CO_2 was supplied after inoculation to closed systems with rubber stoppers by replacing 50% v/v (60 mL) of the headspace with 99.9% v/v CO_2 (AOC Mexico, NL, Mexico) using a syringe.

B. Genome characterization

1) DNA extraction and genome sequencing: DNA was extracted from 60-80 mg frozen biomass pellet using the FastDNA™ Spin Kit for Soil (MP Biomedicals, CA, USA). Sequencing libraries were prepared following the Illumina DNA Prep Protocol and Nextera DNA CD Indexes (Illumina, CA, USA), and the paired-end sequencing run was performed (2x300 bp) using the MiSeq Reagent Kit v3 and the MiSeq Sequencer (Illumina, USA).

2) Genome assembly: De novo genomes were generated using the CLC Workbench Genomics 22.0.2 (Qiagen, USA) program. Firstly, sequencing QC reports were generated, and adaptors and low-quality reads were removed using the Trim Reads tool. Then, genomes were assembled using as parameters 45 for word size, 98 for bubble size and 500 bp as minimum contig length. After, the tool map read to contigs was used and the contig update option was selected to correct errors, and finally, overlapping contigs were merged with the tool align contigs using the paired reads option from the genome finishing module. Assembled genomes were assessed using Quast Genome assembly quality 5.2.0 [41] and Benchmarking Universal Single-Copy Orthologs (BUSCO 5.3.2) [42].

3) Structural and functional annotation: Genomes were annotated using OmicsBox 2.1.14 [43]. For structural annotation, repeat masking tool (Smit, 2013) was conducted utilizing the Hideen Markov Models (HMMER) and the 3041_Chlorophyta database. Followed by the Eukaryotic gene finding analysis with AUGUSTUS 3.4.0 [44] and *Raphidocelis subcapita* as the closest species. RNAseq data from Section II. D was included as extrinsic experimental evidence to identify parts of gene structure and alternative splicing.

4) Functional annotation: Genes were predicted using CDS sequences as queries for BLASTx against the non-redundant protein sequences (nr v5) of viridiplantae, cyanobacteria, rhodophyta, and other phototrophic eukaryote subsets. GO mapping and annotation steps, InterProScan and EggNOG-Mapper were run. Enzyme code (EC) and biochemical pathway were assigned using Kyoto Encyclopedia of Genes and Genomes (KEGG).

C. Microalgae Growth Under Flues Gas

1) Model flue gas: Cement flue gas was simulated according to the exhaust gases from a modern cement plant with a desulfurization system [45], [46]. Flue gas composition consisted of 250 000 ppm CO_2, 700 ppm NO, and 100 ppm SO_2 (in v/v). Cement kiln dust (CKD) was also incorporated into cultures as a strategy to control pH by the addition of 150 mg of CKD dissolved in culture media into the bioreactors daily.

2)Culture medium: A culture medium without nitrogen and sulfur (BG-11-N-S) was used to evaluate the potential of flue gas as a nutrient source. $NaNO_3$ and $MgSO_4 \cdot 6H_2O$ were replaced from the BG-11 medium recipe with NaCl and $MgCl_2.6H_2O$ to provide Mg and Na in the same concentration and preserve solution osmolarity.

3) Experimental conditions in bioreactors: Cultures were performed in a 1 L customized bubble column photobioreactor

(6 cm diameter, 45 cm height) with 980 mL working volume and temperature was controlled by a glass water jacket (Fig 1). Photobioreactor conditions were set at 25 ± 2 °C and continuous illumination with four external fluorescent lamps that provided 80-90 µmol PAR-photons m^{-2} s^{-1} to the vessel's interior. The gas was continuously supplied at a flow rate of 49 mL min^{-1} (0.05 vvm) by a sparger stone at the bottom of the column.

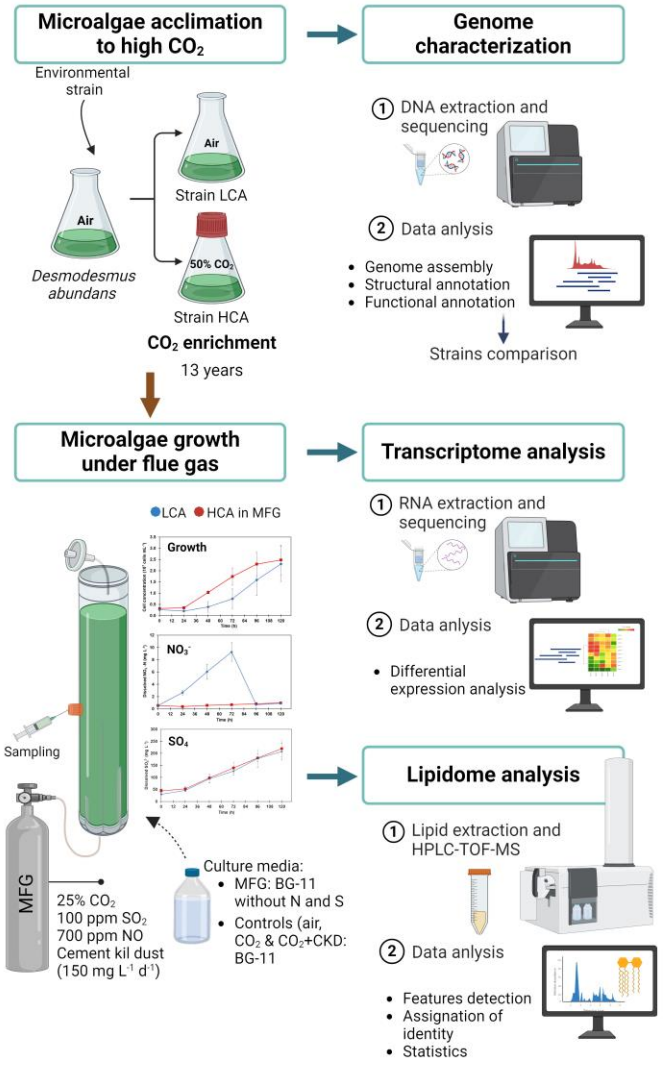

Fig. 1 Experimental strategy for the genetic and biochemical characterization of *D. abundans* strains after 13 of acclimation under high CO_2 and model flue gas (MFG).

D. Transcriptome analysis

1) RNA extraction and RNA-seq: Microalgal biomass samples were harvested at day 4 of growth under flue gas, with three independent replicates for each strain. RNA was extracted from 60-80 mg frozen biomass pellet following the RNeasy Plant Mini Kit (Qiagen, USA) protocol. cDNA libraries were constructed following the TruSeq RNA Sample Prep v2 LS Protocol (Illumina, CA, USA), and the paired-end sequencing run performed (2x81 bp) using the MiSeq Reagent Kit v3 in the MiSeq Sequencer (Illumina, USA).

2) Differential expression analysis: Read quantification and differential analysis were carried out using CLC Workbench Genomics 11.0. Trimmed paired reads were mapped against a generated *de novo* transcriptome and expression tracks were used to identify differentially expressed genes (DEGs) between HCA and LCA strains. P-values were corrected by false discovery rate (FDR) using Benjamini and Hochberg's method. The significance threshold was set at FDR<0.01 and $\log_2$(FC)>2.

E. Lipidome analysis

1) Lipids extraction and High-Performance Liquid Chromatography (HPLC): Samples were harvested at day 4 of growth under flue gas, and lyophilized. Lipid extraction and chromatographic separation were performed as previously described by Mora-Godínez *et al.* [47]. Briefly, cell lysis was performed using 5 mg of dried biomass with 1.5 mL 100 % methanol, 500 µL HPLC water, and 10 glass beads (1 mm diameter) in a FastPrep®-24 Homogenizer (MP Biomedicals, CA, USA) at 6 m s^{-1} for 40 s. Lipids were recovered and purified after several washes with methyl tert-butyl ether, water, and methanol. The organic phase was recovered and evaporated at 55 °C using a CentriVap Concentrator (LABCONCO, MO, USA).

Lipidic extracts were resuspended in isopropanol and analyzed in a HPLC (Series 1100; Agilent, CA, USA) coupled via ESI to a TOF MS Detector (G1969A; Agilent, CA, USA) system. A Luna C18(2) column (150x2 mm, 3 µm; Phenomenex, CA, USA) was used, and mobile phases were (phase A) water:acetonitrile (4:1 v/v) and (phase B) isopropanol:acetonitrile (9:1 v/v), both modified with 10 mM ammonium acetate and 0.1 % formic acid. Elution gradient and HPLC conditions were set as previously reported [47].

3) Feature detection and identity assignation: CDF files were processed with MZmine 2.28. GridMass algorithm was used for peak detection and RANSAC algorithm for feature alignment. Peaks were filtered using 2 as the minimum of peaks in a row; and gap filling with an m/z tolerance of 0.025 (50 ppm). Putative identities were assigned using the Lipid MAPS® database.

III. Results And Discussion

A. Genome characterization of D. abundans strains acclimated to low and high CO_2

Because of the increase of CO_2 emissions and other greenhouse gases, there is a need to look for microalgae strains with high fixation rates, as well as to understand the adaptation mechanisms to high CO_2 and extreme growth

conditions as in flue gas. Therefore, the genome of the *D. abundans* strain HCA, which has been acclimated to high CO_2 for 13 years, was characterized and compared to the strain LCA. The assembled genome of the *D. abundans* strain LCA resulted in an estimated size of 83.61 Mb with 4 174 contigs, and a N50 of 48 590 bp (Table I). Similarly, the HCA strain genome had a size of 81.20 Mb with 4 097 contigs and a N50 of 48 310 bp. Both genomes presented around 91 % BUSCOs of which 85 % corresponded to complete and 5 % to fragmented sequences. However, differences in the number of predicted genes were observed, with 14 251 genes for LCA strain and 10 535 for HCA strain.

TABLE I
STATISTIC PARAMETERS AND COMPLETENESS BASED ON BUSCO ANALYSIS OF THE ASSEMBLED GENOMES OF *D. ABUNDANS* STRAINS HCA AND LCA.

Assembly statistic	HCA	LCA
Genome size (bp)	81 204 747	83 611 544
Total contigs	4 097	4 174
Contig N50 (bp)	48 310	48 590
Largest contig	301 775	303 670
Contigs >= 0 bp	4 098	4 175
Contigs >= 1000 bp	3 583	3 748
GC content (%)	56.62	56.36
Reads mapping (%)	99.46	99.46
N´s per 100 Kbp	1246.34	1742.28
Predicted genes	10 535	14 251
BUSCOs (%)[1]		
Complete	85.6	85.2
Fragmented	5.2	5.5
Missing	9.2	9.3

[1]Includes 1518 BUSCOs from 16 Chlorophyta genomes.

Also, a lower number of sequences with GO term assignations were observed in HCA compared to LCA strain (7 302 versus 8 362), probably due to the lower number of predicted genes. However, a similar number of sequences were assigned annotated in KEGG pathways (5 342). For both strains, the highest represented GO terms were membrane, ATP binding, nucleus, and cytosol (Fig. 2a), still more sequences were present for most of these GO terms in LCA. Differences in the number of predicted and annotated genes between strains could be because genes are identified according to known genes in databases, and the genome of the strain HCA appears to have accumulated many genetic variants that significantly changed the gene sequence, which difficulties the identification of more genes.

After GO terms annotation, genes were assigned to KEGG metabolic pathways (Fig. 2a-b). Specifically, genes involved in carbon fixation and nitrogen metabolism were identified in *D. abundans HCA* and compared to strain LCA (Fig. 3). A total of 22 enzymes from C3 (Calvin-Benson cycle) and C4 (dicarboxylic acid or Hatch and Slack cycle) pathways were found in both strains (Fig. 2a-b). However, different numbers of sequences codifying for some enzymes were found between strains. Among them, D-glyceraldehyde-3-phosphate:NAD+ oxidoreductases (GAPDH, EC 1.2.1.12 and EC 1.2.1.59) with 10 sequences for each enzyme in strain HCA and 8 in LCA; moreover for D-glyceraldehyde-3-phosphate aldose-ketose-isomerase (GAPDH3, EC 5.3.1.1) a higher number of sequences were observed for LCA than HCA (6 and 4, respectively), and with the highest difference phosphate:oxaloacetate carboxy-lyase (PPC) presented 5 sequences for HCA and 2 for LCA strain. On the other hand, for anhydrase carbonic enzyme (CA, EC 4.2.1.1), in strain HCA it was identified half of the sequences number in LCA (Fig. 2c-d). Also, differences were found in nitrate (NR) and nitrite reductases (NiR), as well as in glutamate (GOGAT) and glutamine (GS) synthases, among others.

B. Growth and biomass composition of microalgae strains under flue gas

Both microalgae strains demonstrated the capacity to use flue gas as a nutrient source of C, N, and S. Cement flue gas composition possesses high amounts of CO_2; but also of NO_x, and SO_x that are oxidized to nitrite or nitrate and sulfate in aerobic conditions, and can be used by microalgae [48], [49]. Despite both strains showed a high tolerance to flue gas, HCA presented a higher growth rate during the exponential phase than strain LCA (Table II). By the end of the experimental period, both strains presented similar biomass productivities (0.3 g d.w L^{-1} d^{-1}), probably because of photobioreactor limitations.

On the other hand, the conversion of flue gas components into value-added byproducts is of great interest. Biomass composition analysis showed higher pigment content in strain HCA by 35 % chlorophyll a, 44 % chlorophyll b, and 32 % carotenoids. On the contrary, starch was accumulated in higher quantities in the LCA than HCA strain (23.1 vs 47.2 % d.w.), as well as lipids (9.0 vs 19.1 % d.w.). Since, N was a limited factor under the flue gas condition because of the solubility of NO, we hypothesize that this represented a higher stress for strain LCA, and therefore photosynthates accumulated as storage compounds (starch and lipids), as previously reported [50].

TABLE II
SPECIFIC GROWTH RATE, BIOMASS PRODUCTIVITY AND COMPOSITION OF *D. ABUNDANS* STRAINS UNDER FLUE GAS.

Parameter	Strain HCA	Strain LCA
Specific growth rate (d^{-1})	0.8 ± 0.1	0.6 ± 0.1
Biomass productivity (g d.w L^{-1} d^{-1})	0.3 ± 0.1	0.3 ± 0.1
Chlorophyll a (µg mg^{-1} d.w.)	7.7 ± 0.5^{A}	5.0 ± 0.3^{B}
Chlorophyll b (µg mg^{-1} d.w.)	2.5 ± 0.2^{A}	1.4 ± 0.1^{B}
Carotenoids (µg mg^{-1} d.w.)	2.8 ± 0.2^{A}	1.9 ± 0.1^{B}
Protein (% d.w)	21.3 ± 0.1	21.4 ± 0.5
Starch (%. d.w)	23.1 ± 4.5	47.2 ± 22.3
Lipids (% d.w)	9.0 ± 1.0^{A}	19.1 ± 1.0^{B}

Different letters indicate significant differences between strains (t-test, p. value<0.05).

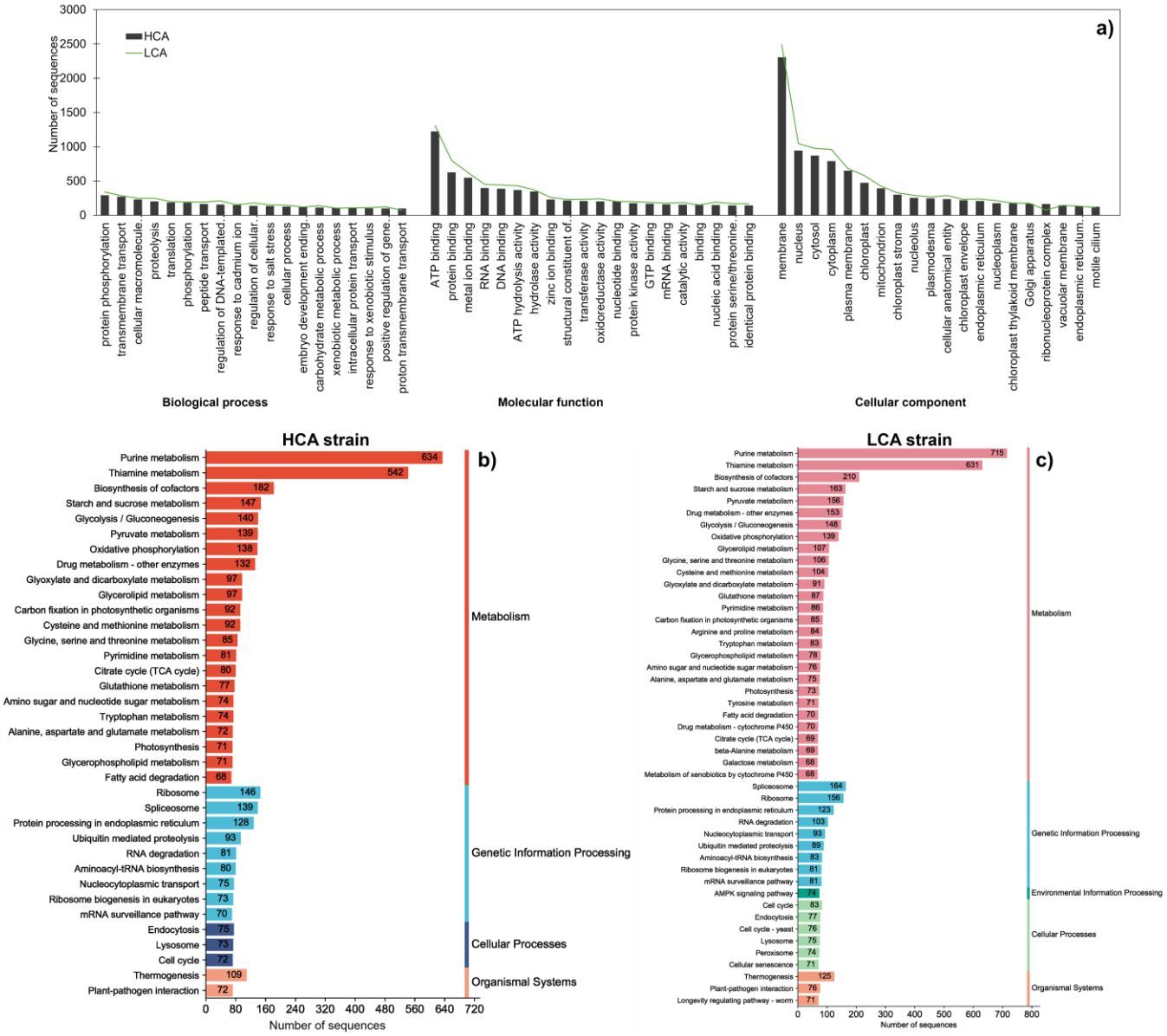

Fig. 2 Functional annotation of *D. abundans* HCA and LCA genomes. Annotation of Gene Ontology (GO) terms (a), and KEGG pathway assignations of *D. abundans* HCA (b) and LCA (c) genomes.

C. Differential expressed genes of CO_2 fixation pathways and concentration mechanisms in D. abundans strains under flue gas

Strains adaptative changes to high CO_2 were also studied at gene expression level. Transcriptome analysis resulted in high up-regulated contigs (16 435 vs. 4 2.19 down-regulated) in the HCA strain compared to the LCA strain, both under flue gas. Table III showed differentially expressed genes encoding for enzymes of CO_2 concentration mechanisms (CCM), C3 and C4 cycles, which are also represented in Fig. 3. Several contigs for most enzymes were observed for HCA and LCA, probably due to differential preference of gene isoforms. However, since these high numbers of variable contigs were observed from the genome where several sequences were found for an enzyme, it is suggested that the strains acquired genome changes during the acclimation strategy.

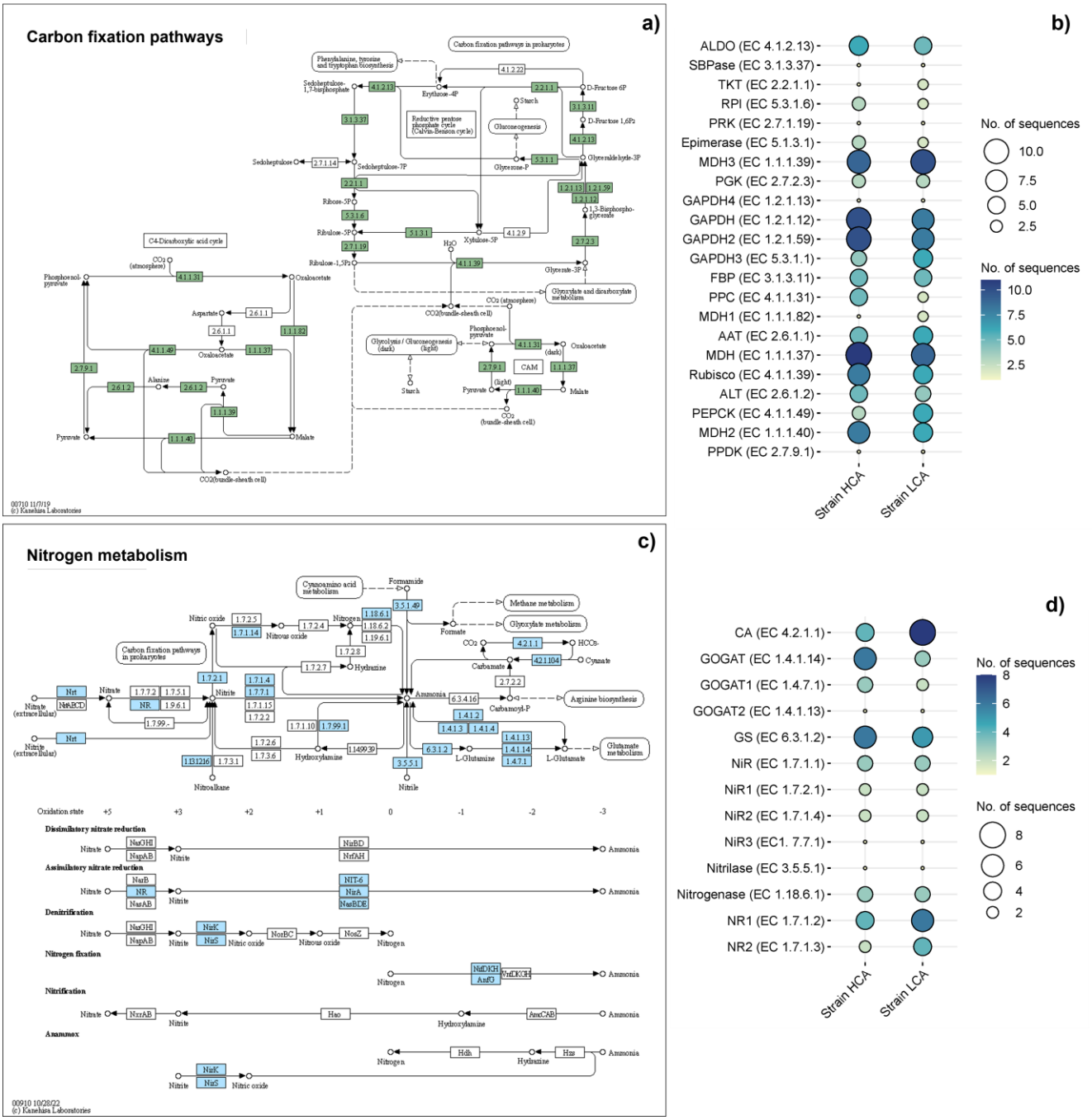

Fig. 3 Carbon fixation (a-b) and nitrogen metabolism (c-d) pathways in *D. abundans* strains HCA and LCA. The abundance of key genes strain genomes in each strain is represented by the dot size and color intensity (b, c).

In this study, some components of the CO_2 concentration mechanism (CCM) were up-regulated in the HCA strain under high CO_2 (Table III). However, the CCM is normally down-regulated under high CO_2 [51]. Putative carbonic anhydrases (CAs) possess conserved regions of the alpha-type family, that are associated with constitutive expression [51]. Therefore, this suggests that CAs probably keep active to assist other metabolic pathways, but also to use the different forms of inorganic carbon in the medium (CO_2 and HCO_3^-).

Several pathways of central carbon metabolism were up-regulated in the HCA strain compared to the LCA strain (Table III). For example, in the C3 cycle, several contigs were observed for most enzymes. Of these, most up-regulated contigs were found a higher magnitude of change than those down-regulated.

TABLE III
DIFFERENTIALLY EXPRESSED GENES ASSOCIATED WITH CARBON FIXATION PATHWAYS IN *D. ABUNDANS* STRAINS UNDER FLUE GAS.

Pathway	Enzyme Name	Enzyme Code (EC)	DEGs Log$_2$FC	DEGs FDR
Carbon concentrating mechanisms (CCM)	Carbonic anhydrase	4.2.1.1	9.75	0.0003
			10.59	0.0001
			-8.51	0.0026
			10.55	0.0000
			7.94	0.0035
			7.64	0.0048
			-6.59	0.0000
			-4.65	0.0021
CO_2 fixation	Ribulose-biphosphate carboxylase	4.1.1.39	12	0.0000
			-6.96	0.0000
			8.41	0.0024
			7.72	0.0044
C3 cycle	Phosphoglycerate kinase	2.7.2.3	13.35	0.0000
			-7.12	0.0000
			3.13	0.0000
			8.34	0.0021
	Glyceraldehyde 3-PO_4 dehydrogenase	1.2.1.12, 1.2.1.59	14.22	0.0000
			-7.16	0.0000
			11.75	0.0000
			4.01	0.0000
	Glyceraldehyde 3-PO_4 dehydrogenase (NADP+) (Phosphorylating)	1.2.1.13, 1.2.1.59	12.56	0.0000
			-3.25	0.0000
	Transketolase	2.2.1.1	13.37	0.0000
			-7.50	0.0000
	Ribose-5-phosphate isomerase	5.3.1.6	13.12	0.0000
			-6.70	0.0000
	Phosphoribulokinase	2.7.1.19	15.10	0.0000
			-7.26	0.0000
C4 cycle	Phosphoenolpyruvate carboxylase	4.1.1.31	-5.57	0.0000
			11.80	0.0000
			12.14	0.0000
			-6.79	0.0000
	Aspartate aminotransferase	2.6.1.1	-5.64	0.0000
			3.59	0.0000
			11.03	0.0000
			7.63	0.0054
			-5.03	0.0000
			8.00	0.0031
	Malate dehydrogenase	1.1.1.37	-7.03	0.0000
			10.79	0.0000
			-13.85	0.0000
			11.51	0.0001
			14.17	0.0000
			-8.33	0.0027
			11.42	0.0000
			11.75	0.0000
			-6.58	0.0000
	Malate dehydrogenase (NADP+)	1.1.1.82	-7.28	0.0096
			12.27	0.0000
	Malate dehydrogenase (Oxaloacetate-decarboxylating) (NADP+)	1.1.1.40	-4.77	0.0000
			9.51	0.0004
			7.94	0.0034
			8.89	0.0000
	Malate dehydrogenase (decarboxylating)	1.1.1.39	11.70	0.0000
			-5.82	0.0001
			9.73	0.0003
			7.26	0.0076
	Phosphoenolpyruvate carboxykinase (ATP)	4.1.1.49	13.65	0.0000
			-10.79	0.0001
			8.44	0.0019
			12.22	0.0000
	Alanine transaminase	2.6.1.2	10.19	0.0000
			-7.08	0.0000
			9.11	0.0007
	Pyruvate -phosphate dikinase	2.7.9.1	12.71	0.0000
			-7.34	0.0000

D. Lipidome analysis of D. abundans strains *under flue gas*

Principal component analysis separated LCA replicates from HCA by principal component 1 which explained 88.8% of data variability (Fig. 4a). Lipid profiles showed higher glycerolipid intensities in strain LCA than HCA, while glycerophospholipids were increased in HCA (Fig. 4b). As previously explained, results suggest that flue gas represented a more stressful condition for the LCA strain since under optimal conditions, fatty acids are synthesized and used to generate membrane lipids [14], [52], [53], while under stress, glycerolipids are accumulated [54]. Data correlates with a higher growth rate observed at the beginning of the experiment for the HCA strain (Table II).

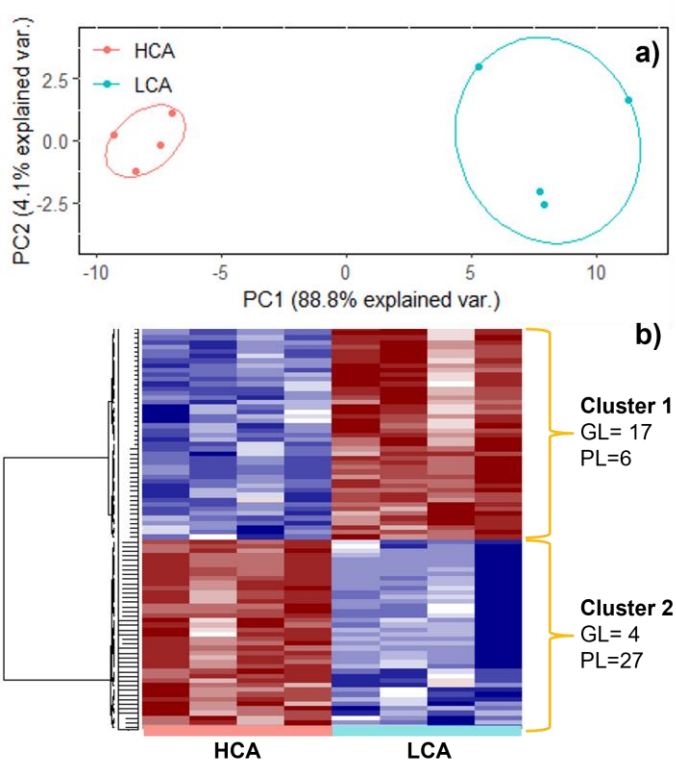

Fig. 4 Lipidome analysis of *D. abundans* strains HCA and LCA under flue gas. a) Principal component analysis. b) Heatmap of significant changing features (t-test, FDR<0.05).

IV. CONCLUSIONS

In this study, draft genomes for two strains of *D. abundans* were generated and characterized. Transcriptome revealed several differentially expressed genes between strains. Specifically, genes associated with carbon fixation pathways suggested a higher internal carbon flux and a better strategy to scavenge N for the HCA strain. In accordance, increased intensities of putative glycerophospholipids, but lower glycerolipid intensities in strain HCA might evidence an active growth with fewer lipid reserves, as confirmed by the biochemical analysis. Results suggest that *D. abundans* strains possess different levels of adaptability and response to flue gas as consequence of the acclimation to different CO_2 concentrations for 13 years. Understanding the adaptative mechanisms to high CO_2 and response to flue gas conditions could contribute to developing cultivation strategies for the

establishment of sustainable CO_2 mitigation and biotechnology applications.

ACKNOWLEDGMENT

The authors would like to acknowledge Centro de Biotecnología FEMSA, Tecnologico de Monterrey, for their support with laboratory facilities; and to CONAHCYT for doctoral scholarship to author S.M.-G (no. 827922).

REFERENCES

[1] IPCC, "Climate Change 2022: Impacts, Adaptation and Vulnerability. Contribution of Working Group II to the Sixth Assessment Report of the Intergovernmental Panel on Climate Change. H.-O. Pörtner, D.C. Roberts, M. Tignor, E.S. Poloczanska, K. Mintenbeck, A. Alegría, M. Craig, S. Langsdorf, S. Löschke, V. Möller, A. Okem, B. Rama". Cambridge, UK and New York, USA, 2022.

[2] WMO & GAW, "WMO Greenhouse Gas Bulletin - No. 18: The State of Greenhouse Gases in the Atmosphere Based on Global Observations through 2021," 2022.

[3] C. Sepulveda, C. Gómez, N. El Bahraoui, and G. Acién, "Comparative evaluation of microalgae strains for CO 2 capture purposes," *Journal of CO2 Utilization*, vol. 30, pp. 158–167, Mar. 2019, doi: 10.1016/j.jcou.2019.02.004.

[4] J. Fan et al., "Impacts of CO2 concentration on growth, lipid accumulation, and carbon-concentrating-mechanism-related gene expression in oleaginous *Chlorella*," *Appl Microbiol Biotechnol*, vol. 99, no. 5, pp. 2451–2462, Feb. 2015, doi: 10.1007/s00253-015-6397-4.

[5] B. L. Chen, W. Mhuantong, S. H. Ho, J. S. Chang, X. Q. Zhao, and F. W. Bai, "Genome sequencing, assembly, and annotation of the self-flocculating microalga *Scenedesmus obliquus* AS-6-11," *BMC Genomics*, vol. 21, no. 1, Dec. 2020, doi: 10.1186/s12864-020-07142-4.

[6] H. R. Molitor and J. L. Schnoor, "Using simulated flue gas to rapidly grow nutritious microalgae with enhanced settleability," *ACS Omega*, vol. 5, no. 42, pp. 27269–27277, Oct. 2020, doi: 10.1021/acsomega.0c03492.

[7] United Nations, "The Sustainable Development Goals Report," 2022.

[8] R. Barten et al., "Genetic mechanisms underlying increased microalgal thermotolerance, maximal growth rate, and yield on light following adaptive laboratory evolution," *BMC Biol*, vol. 20, no. 1, Dec. 2022, doi: 10.1186/s12915-022-01431-y.

[9] M. Premaratne, V. C. Liyanaarachchi, G. K. S. H. Nishshanka, P. H. V. Nimarshana, and T. U. Ariyadasa, "Nitrogen-limited cultivation of locally isolated Desmodesmus sp. For sequestration of CO2 from simulated cement flue gas and generation of feedstock for biofuel production," *J Environ Chem Eng*, vol. 9, no. 4, Aug. 2021, doi: 10.1016/j.jece.2021.105765.

[10] H. Sun, W. Zhao, X. Mao, Y. Li, T. Wu, and F. Chen, "High-value biomass from microalgae production platforms: Strategies and progress based on carbon metabolism and energy conversion," *Biotechnology for Biofuels*, vol. 11, no. 1. BioMed Central Ltd., Aug. 20, 2018. doi: 10.1186/s13068-018-1225-6.

[11] V. T. Duong, F. Ahmed, S. R. Thomas-Hall, S. Quigley, E. Nowak, and P. M. Schenk, "High protein- and high lipid-producing microalgae from northern Australia as potential feedstock for animal feed and biodiesel," *Front Bioeng Biotechnol*, vol. 3, 2015, doi: 10.3389/fbioe.2015.00053.

[12] X. M. Sun, L. J. Ren, Q. Y. Zhao, X. J. Ji, and H. Huang, "Microalgae for the production of lipid and carotenoids: A review with focus on stress regulation and adaptation," *Biotechnology for Biofuels*, vol. 11, no. 1. BioMed Central Ltd., Oct. 04, 2018. doi: 10.1186/s13068-018-1275-9.

[13] G. Muhammad et al., "Modern developmental aspects in the field of economical harvesting and biodiesel production from microalgae biomass," *Renewable and Sustainable Energy Reviews*, vol. 135. Elsevier Ltd, Jan. 01, 2021. doi: 10.1016/j.rser.2020.110209.

[14] L. Yao, J. A. Gerde, S. L. Lee, T. Wang, and K. A. Harrata, "Microalgae lipid characterization," *J Agric Food Chem*, vol. 63, no. 6, pp. 1773–1787, Feb. 2015, doi: 10.1021/jf5050603.

[15] A. Ghosh et al., "Progress toward isolation of strains and genetically engineered strains of microalgae for production of biofuel and other value added chemicals: A review," *Energy Conversion and Management*, vol. 113. Elsevier Ltd, pp. 104–118, Apr. 01, 2016. doi: 10.1016/j.enconman.2016.01.050.

[16] Y. Guo et al., "Metabolic acclimation mechanism in microalgae developed for CO2 capture from industrial flue gas," *Algal Res*, vol. 26, pp. 225–233, Sep. 2017, doi: 10.1016/j.algal.2017.07.029.

[17] V. C. Liyanaarachchi, M. Premaratne, T. U. Ariyadasa, P. H. V. Nimarshana, and A. Malik, "Two-stage cultivation of microalgae for production of high-value compounds and biofuels: A review," *Algal Res*, vol. 57. Elsevier B.V., Jul. 01, 2021. doi: 10.1016/j.algal.2021.102353.

[18] C. Ye et al., "Life cycle assessment of industrial scale production of spirulina tablets," *Algal Res*, vol. 34, pp. 154–163, Sep. 2018, doi: 10.1016/j.algal.2018.07.013.

[19] F. G. Acién Fernández, J. M. Fernández Sevilla, and E. Molina Grima, "Costs analysis of microalgae production," in *Biofuels from Algae*, Elsevier, 2019, pp. 551–566. doi: 10.1016/b978-0-444-64192-2.00021-4.

[20] N. Rafa, S. F. Ahmed, I. A. Badruddin, M. Mofijur, and S. Kamangar, "Strategies to Produce Cost-Effective Third-Generation Biofuel From Microalgae," *Frontiers in Energy Research*, vol. 9. Frontiers Media S.A., Sep. 07, 2021. doi: 10.3389/fenrg.2021.749968.

[21] R. García-Cubero, J. Moreno-Fernández, and M. García-González, "Modelling growth and CO2 fixation by *Scenedesmus vacuolatus* in continuous culture," *Algal Res*, vol. 24, pp. 333–339, Jun. 2017, doi: 10.1016/j.algal.2017.04.018.

[22] W. J. Henley, "The past, present and future of algal continuous cultures in basic research and commercial applications," *Algal Research*, vol. 43. Elsevier B.V., Nov. 01, 2019. doi: 10.1016/j.algal.2019.101636.

[23] J. F. López-Hernández, P. García-Alamilla, D. Palma-Ramírez, C. A. Álvarez-González, J. C. Paredes-Rojas, and F. J. Márquez-Rocha, "Continuous microalgal cultivation for antioxidants production," *Molecules*, vol. 25, no. 18, Sep. 2020, doi: 10.3390/molecules25184171.

[24] B. Zhang, J. Wu, and F. Meng, "Adaptive Laboratory Evolution of Microalgae: A Review of the Regulation of Growth, Stress Resistance, Metabolic Processes, and Biodegradation of Pollutants," *Frontiers in Microbiology*, vol. 12. Frontiers Media S.A., Aug. 18, 2021. doi: 10.3389/fmicb.2021.737248.

[25] M. M. Perrineau et al., "Using natural selection to explore the adaptive potential of *Chlamydomonas reinhardtii*," *PLoS One*, vol. 9, no. 3, Mar. 2014, doi: 10.1371/journal.pone.0092533.

[26] S. Calhoun et al., "A multi-omic characterization of temperature stress in a halotolerant *Scenedesmus* strain for algal biotechnology," *Commun Biol*, vol. 4, no. 1, Dec. 2021, doi: 10.1038/s42003-021-01859-y.

[27] E. R. Hanschen and S. R. Starkenburg, "The state of algal genome quality and diversity," *Algal Res*, vol. 50. Elsevier B.V., Sep. 01, 2020. doi: 10.1016/j.algal.2020.101968.

[28] M. I. S. Naduthodi, N. J. Claassens, S. D'Adamo, J. van der Oost, and M. J. Barbosa, "Synthetic Biology Approaches To Enhance Microalgal Productivity," *Trends in Biotechnology*, vol. 39, no. 10. Elsevier Ltd, pp. 1019–1036, Oct. 01, 2021. doi: 10.1016/j.tibtech.2020.12.010.

[29] M. Cecchin et al., "Molecular basis of autotrophic vs mixotrophic growth in *Chlorella sorokiniana*," *Sci Rep*, vol. 8, no. 1, Dec. 2018, doi: 10.1038/s41598-018-24979-8.

[30] J. Yang, C. Zhang, and H. Hu, "Screening High CO2-Tolerant Oleaginous Microalgae from Genera *Desmodesmus* and *Scenedesmus*," *Appl Biochem Biotechnol*, vol. 192, no. 1, pp. 211–229, Sep. 2020, doi: 10.1007/s12010-020-03319-5.

[31] A. Solovchenko and I. Khozin-Goldberg, "High-CO2 tolerance in microalgae: Possible mechanisms and implications for biotechnology and bioremediation," *Biotechnology Letters*, vol. 35, no. 11. pp. 1745–1752, Nov. 2013. doi: 10.1007/s10529-013-1274-7.

[32] L. Patil and B. Kaliwal, "Effect of CO2 Concentration on Growth and Biochemical Composition of Newly Isolated Indigenous Microalga *Scenedesmus bajacalifornicus* BBKLP-07," *Appl Biochem Biotechnol*, vol. 182, no. 1, pp. 335–348, May 2017, doi: 10.1007/s12010-016-2330-2.

[33] S. Wang et al., "The Draft Genome of the Small, Spineless Green Alga *Desmodesmus costato-granulatus* (Sphaeropleales, Chlorophyta)," *Protist*, vol. 170, no. 6, Dec. 2019, doi: 10.1016/j.protis.2019.125697.

[34]E. P. Knoshaug, A. Nag, D. P. Astling, D. Douchi, and L. M. L. Laurens, "Draft Genome Sequence of the Biofuel-Relevant Microalga *Desmodesmus armatus*," *Microbiol Resour Announc*, vol. 9, no. 6, Feb. 2020, doi: 10.1128/mra.00896-19.

[35]C. Nag Dasgupta, S. Nayaka, K. Toppo, A. K. Singh, U. Deshpande, and A. Mohapatra, "Draft genome sequence and detailed characterization of biofuel production by oleaginous microalga *Scenedesmus quadricauda* LWG002611 06 Biological Sciences 0604 Genetics," *Biotechnol Biofuels*, vol. 11, no. 1, Nov. 2018, doi: 10.1186/s13068-018-1308-4.

[36]S. R. Starkenburg et al., "Draft nuclear genome, complete chloroplast genome, and complete mitochondrial genome for the biofuel/ bioproduct feedstock species *Scenedesmus obliquus* strain DOE0152z," *Genome Announc*, vol. 5, no. 32, Aug. 2017, doi: 10.1128/genomeA.00617-17.

[37]T. J. Yeh et al., "Transcriptome and physiological analysis of a lutein-producing alga *Desmodesmus sp*. reveals the molecular mechanisms for high lutein productivity," *Algal Res*, vol. 21, pp. 103–119, Jan. 2017, doi: 10.1016/j.algal.2016.11.013.

[38]R. Wang, P. Diao, Q. Chen, H. Wu, N. Xu, and S. Duan, "Identification of novel pathways for biodegradation of bisphenol A by the green alga *Desmodesmus sp.* WR1, combined with mechanistic analysis at the transcriptome level," *Chemical Engineering Journal*, vol. 321, pp. 424–431, 2017, doi: 10.1016/j.cej.2017.03.121.

[39]A. Sirikhachornkit, A. Suttangkakul, S. Vuttipongchaikij, and P. Juntawong, "De novo transcriptome analysis and gene expression profiling of an oleaginous microalga Scenedesmus acutus TISTR8540 during nitrogen deprivation-induced lipid accumulation," *Sci Rep*, vol. 8, no. 1, Dec. 2018, doi: 10.1038/s41598-018-22080-8.

[40]J. A. Lara-Gil, M. M. Álvarez, and A. Pacheco, "Toxicity of flue gas components from cement plants in microalgae CO2 mitigation systems," *J Appl Phycol*, vol. 26, no. 1, pp. 357–368, Feb. 2014, doi: 10.1007/s10811-013-0136-y.

[41]A. Gurevich, V. Saveliev, N. Vyahhi, and G. Tesler, "QUAST: quality assessment tool for genome assemblies," *Bioinformatics*, vol. 29, no. 8, pp. 1072–1075, Apr. 2013, doi: 10.1093/bioinformatics/btt086.

[42]F. A. Simão, R. M. Waterhouse, P. Ioannidis, E. V. Kriventseva, and E. M. Zdobnov, "BUSCO: assessing genome assembly and annotation completeness with single-copy orthologs," *Bioinformatics*, vol. 31, no. 19, pp. 3210–3212, Oct. 2015, doi: 10.1093/bioinformatics/btv351.

[43]BioBam Bioinformatics, "OmicsBox - Bioinformatics made easy." 2019.

[44]K. J. Hoff and M. Stanke, "Predicting Genes in Single Genomes with AUGUSTUS," *Curr Protoc Bioinformatics*, p. e57, Nov. 2018, doi: 10.1002/cpbi.57.

[45]EEA, "EMEP/EEA air pollutant emission inventory guidebook 2019," 2019.

[46]wbscd, "Guidelines for Emissions Monitoring and Reporting in the Cement Industry. Emissions Monitoring and Reporting. Version 2.0," 2012.

[47]S. Mora-Godínez, C. E. Rodríguez-López, C. Senés-Guerrero, V. Treviño, R. Díaz De La Garza, and A. Pacheco, "Effect of high CO2concentrations on Desmodesmus abundans RSM lipidome," *Journal of CO2 Utilization*, vol. 65, Nov. 2022, doi: 10.1016/j.jcou.2022.102183.

[48]J. A. Lara-Gil, C. Senés-Guerrero, and A. Pacheco, "Cement flue gas as a potential source of nutrients during CO2 mitigation by microalgae," *Algal Res*, vol. 17, pp. 285–292, Jul. 2016, doi: 10.1016/j.algal.2016.05.017.

[49]E. Van Eynde, B. Lenaerts, T. Tytgat, R. Blust, and S. Lenaerts, "Valorization of Flue Gas by Combining Photocatalytic Gas Pretreatment with Microalgae Production," *Environ Sci Technol*, vol. 50, no. 5, pp. 2538–2545, Mar. 2016, doi: 10.1021/acs.est.5b04824.

[50]K. W. M. Tan, H. Lin, H. Shen, and Y. K. Lee, "Nitrogen-induced metabolic changes and molecular determinants of carbon allocation in *Dunaliella tertiolecta*," *Sci Rep*, vol. 6, Nov. 2016, doi: 10.1038/srep37235.

[51]Y. Wang, D. J. Stessman, and M. H. Spalding, "The CO2 concentrating mechanism and photosynthetic carbon assimilation in limiting CO2: How *Chlamydomonas* works against the gradient," Plant Journal, vol. 82, no. 3, pp. 429–448, May 2015, doi: 10.1111/tpj.12829.

[52]H. Rismani-Yazdi, B. Z. Haznedaroglu, K. Bibby, and J. Peccia, "Transcriptome sequencing and annotation of the microalgae *Dunaliella tertiolecta*: Pathway description and gene discovery for production of next-generation biofuels," *BMC Genomics*, vol. 12, Mar. 2011, doi: 10.1186/1471-2164-12-148.

[53]Y. F. Niu et al., "Improvement of neutral lipid and polyunsaturated fatty acid biosynthesis by overexpressing a type 2 diacylglycerol acyltransferase in marine diatom *Phaeodactylum tricornutum*," *Mar Drugs*, vol. 11, no. 11, pp. 4558–4569, 2013, doi: 10.3390/md11114558.

[54]Z. Sun, Y. F. Chen, and J. Du, "Elevated CO2 improves lipid accumulation by increasing carbon metabolism in *Chlorella sorokiniana*," *Plant Biotechnol J*, vol. 14, no. 2, pp. 557–566, Feb. 2016, doi: 10.1111/pbi.12398.